### Title

Regime shift of the hydroclimatevegetation system in the Yellow River Delta of China from 1982 through 2015




### Journal

Environmental Research Letters, 15(2)

### ISSN

1748-9318



### Authors

Niu, Beibei

Zhang, Zixuan

Yu, Xinyang

et al.



### Publication Date

2020-02-01

### DOI

10.1088/1748-9326/ab6561

Peer reviewed

ENVIRONMENTAL RESEARCH
LETTERS



LETTER • OPEN ACCESS

# Regime shift of the hydroclimate–vegetation system in the Yellow River Delta of China from 1982 through 2015

To cite this article: Beibei Niu *et al* 2020 *Environ. Res. Lett.* **15** 024017

Environmental Research Letters

LETTER

# Regime shift of the hydroclimate–vegetation system in the Yellow River Delta of China from 1982 through 2015

**Beibei Niu**[1], **Zixuan Zhang**[1], **Xinyang Yu**[1], **Xinju Li**[1,5], **Zhen Wang**[2], **Hugo A Loáiciga**[3] **and Sha Peng**[4]

[1] College of Resources and Environment, Shandong Agricultural University, Taian 271018, People's Republic of China
[2] School of Resource & Environmental Sciences, Wuhan University, Wuhan 430079, People's Republic of China
[3] Department of Geography, University of California, Santa Barbara, CA 93106, United States of America
[4] School of Low Carbon Economics, Hubei University of Economics, Wuhan 430205, People's Republic of China
[5] Author to whom any correspondence should be addressed.

**E-mail:** xinjuli@sdau.edu.cn

**OPEN ACCESS**

**RECEIVED**
4 May 2019

**REVISED**
20 October 2019

**ACCEPTED FOR PUBLICATION**
24 December 2019

**PUBLISHED**
7 February 2020

**Keywords:** regime shift, hydroclimate–vegetation system, time series decomposition, structural change, Yellow River Delta

Supplementary material for this article is available online



## Abstract

The Yellow River Delta (YRD) has been experiencing substantial climatic, hydrological, and anthropogenic stresses, and a sound understanding of the regime shift in its hydroclimate–vegetation system is of fundamental importance for maintaining the health and stability of its regional ecosystems. This study constructs and analyzes a 34-year-dataset (1982–2015) of hydro–climatic variables and satellite-based Normalized Difference Vegetation Index (NDVI) in the YRD. A seasonal-trend decomposition technique based on loess (STL), and a structural change analysis were coupled to detect regime shifts of regional hydroclimate and vegetation in the YRD from 1982 through to 2015. During this period the YRD exhibited a significant warmer–drier–greening trend and experienced four regime shifts of its hydroclimate–vegetation system, with the four shift periods roughly centered in 1989, 1998, 2004, and 2012. Partial correlation analysis revealed that temperature was the dominant factor promoting vegetative growth in spring and autumn (all $P_{NDVI\text{-}TEM}$ greater than 0.65), and streamflow impacted the NDVI mainly in summer. Temperature and precipitation were the dominant controls of vegetative growth during the growing season prior to 2002, and thereafter precipitation and streamflow alternately became the main moisture-influencing factors of vegetative growth. Streamflow played an important complementary role on vegetative growth, particularly in near riverine areas when drought exceeds a certain threshold. Additionally, climate shifts determined the changing trend of NDVI across the region, while the effect of land use change is localized and predominant in the northeastern part of the study region. These findings offer an insight into appropriate water regulation of the Yellow River and on climatic adaptation within the YRD.

## 1. Introduction

Understanding environmental change in river deltas is especially important because they are among the world's most altered ecosystems, yet have high socio–ecological interdependence and highly contested resource management and allocation (Hagenlocher *et al* 2018, Liu *et al* 2018a). The Yellow River Delta (YRD) is one of the three largest deltas in China. It is rich in natural resources and contains important wetland ecosystems, providing important habitats for rare and endangered bird species (Zhou *et al* 2015, Lu *et al* 2016). In recent decades the hydrologic regime of the YRD has been altered by dramatic climatic and anthropogenic changes in the Yellow River Basin, thus increasing the vulnerability of its deltaic system (Jiang *et al* 2017). Notorious among the factors of change was the construction of the Xiaolangdi Reservoir, which intercepts streamflow and has reduced the water and sediment discharging into the YRD (Wei *et al* 2016). The resulting modifications to the YRD include changes to its morphology, biodiversity, wetland landscape, and vegetation dynamics (Jiang *et al* 2013, Kong *et al* 2015, Hua *et al* 2016).

Vegetation plays a central role in stabilizing the Earth ecosystem and maintaining human environments (Zhu and Southworth 2013, Hu and Xia 2019, Chu *et al* 2019). Vegetation dynamics constitute a sensitive indicator for the status of ecosystems and are closely related to climate change, hydrological regime, and human activities (John *et al* 2013, Guo *et al* 2017, Wen *et al* 2017). Thus, increasing attention is being paid to detect the effect of hydroclimate on vegetation status at various spatial and temporal scales (Koster *et al* 2014, Xu *et al* 2017, Groß *et al* 2018). Yet, most studies have focused on interpreting the vegetation dynamics induced by changes of specific elements (e.g., water conditions, hydrological disturbances, temperature, and precipitation) (Jiapaer *et al* 2015, Shi *et al* 2017). Less attention has been given to taking climate, hydrology, and vegetation as systems to analyze their overall changes.

Climate, hydrology, and vegetation interact to maintain system stability with varying degrees of resistance/resilience, while internal gradual change and external disturbances trigger ecosystems to cross state thresholds with ensuing regime shifts (Harrison 1979, Walker and Salt 2006, Liu *et al* 2018b). Meanwhile, the patterns of interactions would also change radically with systemic regime shift and rapid reconfiguration, and the new regime requires modified management goals and measures. Therefore, a complete understanding of the regime shift of the hydroclimate–vegetation system in the YRD, particularly the distinct influence patterns of hydroclimate on vegetation in different regimes, is of fundamental importance for managers and policy makers.

This study relies on long-term time series data (1982–2015) of hydro–climatic variables (temperature, precipitation, and streamflow) and satellite-based Normalized Difference Vegetation Index (NDVI) to identify the regime shifts of the hydroclimate–vegetation system in the Yellow River Delta. Regime shift is herein defined as abrupt changes on the mean levels of these variables. Our specific objectives include: (1) detection of regime shift in the regional hydroclimate–vegetation system within the YRD during 1982–2015, and exploring the shift in influence patterns of hydroclimate on vegetation dynamics; (2) discerning the spatial variation of NDVI associated with shifting regimes and assessing the impact of land use changes on NDVI variation. The findings of this study will contribute to the identification of effective water resource management, and climatic adaptation practices in the YRD.

## 2. Data and methods

### 2.1. Study area

The YRD is situated in the northern Shandong Province in eastern China, facing the Bohai Sea in the north and bordering Laizhou Bay in the east. The study area of this work is within Dongying City, which lies between 37°16′ to 38°0′ N and 118°06′ to 119°18′ E, encompassing an area of slightly more than 6,000 km$^2$ (figure 1) and covering much of the YRD. The YRD region is characterized by a warm–temperate, continental monsoonal climate with distinct seasons. Annual average temperature ranges from 11.85 to 14.43 °C, and average annual precipitation equaled 530 mm during 1982–2015. The mean annual potential evaporation is greater than 1,500 mm, with annual average ratio of potential evaporation to precipitation equal to 3.22 (Liu *et al* 2018c). The terrain is gently sloping, with most parts below 10 m in elevation above mean sea level. The groundwater has an average depth of 1.14 m below ground surface with a high degree of mineralization (Fan *et al* 2012). As a result, the soil is typically saline alluvial, with low nutrient content and high salinity (Yu *et al* 2010). Most of the natural vegetation in the area consists of salt tolerant herbs, grasses, and shrubs. The dominant species include *Phragmites australis, Suaeda heteroptera, Tamarix chinensis, Triarrhena sacchariflora, Myriophyllum spicatum, Limonium sinense* (Jiang *et al* 2013).

### 2.2. Data sources and preprocessing

We relied on the GIMMS3g NDVI dataset to assess vegetation dynamics of the YRD. The GIMMS3g is the longest term NDVI dataset to date, derived from the Advanced Very High Resolution Radiometer sensors aboard the National Oceanographic and Atmospheric Administration (NOAA) satellites. Despite its relatively coarse spatial resolution these data correspond well with data captured with higher resolution sensors such as MODIS and SPOT (Fensholt *et al* 2006, Fensholt and Proud 2012). The GIMMS3g data set is therefore generally perceived as the most accurate multi-decadal NDVI dataset (Ibrahim *et al* 2015, Burrell *et al* 2017). The latest version of the GIMMS NDVI3g.v1 data, available at https://ecocast.arc.nasa.gov/data/pub/gimms/3g.v1/, spans the period July 1981 through December 2015, with bi-weekly temporal and 8 km spatial resolutions. Data from January 1982 through December 2015 were downloaded for analysis. The bi-monthly data were converted to monthly aggregates using the maximum value composite method to minimize the influence of atmospheric effects, scan angle, and cloud contamination (Holben 1986). The data corresponding to the spatial extent of the study area were extracted separately and the monthly NDVI dataset of the YRD during 1982–2015 was created in this manner.

The Gridded Dataset (0.5°×0.5°) of Monthly Surface Precipitation of China (V2.0) and Gridded Dataset (0.5° × 0.5°) of Monthly Surface Temperature of China (V2.0), both with a long-time span from 1961 to the present, were obtained from National Meteorological Information Center of China (http://www.nmic.cn/). Then the gridded data with good areal

coverage within the YRD were separately averaged and formed a new dataset of monthly area-averaged precipitation (PRE) and temperature (TEM) of the YRD during 1982–2015, which were used to analyze the climate changes in YRD and their relation with NDVI variations.

The Lijin hydrological station, located approximately 100 km upstream from the river mouth (figure 1), was the station in the YRD employed for monitoring the water-sediment delivery characteristic of the Yellow River. The monthly streamflow (STF) data at the Lijin station during 1982–2015 were gathered from the Yellow River Conservancy Commission.

Three land use datasets of China (1980, 2000, and 2015) with a spatial resolution of 1 km × 1 km were obtained from the Resources and Environmental Sciences Data Center, Chinese Academy of Sciences (http://www.resdc.cn). Land uses were divided into six categories, including cultivated land, forest, grassland, water bodies, built-up land, and unused land. The land use sub-dataset of the YRD was separately extracted to represent the evolution of land use in the YRD during the study period.

### 2.3. Data analysis

#### *2.3.1. Trend analysis*

The overall trends of TEM, PRE, STF and NDVI during 1982–2015 were first calculated using the nonparametric Seasonal Kendall test (Hirsch and Slack 1984), which is insensitive to seasonality, outliers, missing data, and non-normality of the time series (Sarkkola *et al* 2009). The Sen Slope estimation method was used to discover trends in the time series within the seasonal Kendall test.

#### *2.3.2. Regime shift detection*

A seasonal-trend decomposition technique based on loess (STL), and a structural change methodology were coupled to detect regime shifts of the regional hydro-climate–vegetation system in the YRD from 1982 through 2015. The STL is a filtering procedure that applies repeated loess fitting to decompose monthly (or other duration) time series data into smoothed trend, seasonal, and residual components (Cleveland *et al* 1990, Stow *et al* 2015). The trend component represents the long-term processes that operate over the time period, which can contain abrupt system-related changes (Lafare *et al* 2015), while the seasonal fluctuation and shorter-term event related residuals blur important movements and hinder the interpretation of a series. In this regard, the time series of TEM, PRE, STF and NDVI were separately decomposed using STL to extract trend component series, which were, in turn, examined with a structural change algorithm under the most commonly investigated regime shift hypothesis, i.e., a step change in the mean level (Andersen *et al* 2009). This methodology estimates breakpoints and their associated confidence intervals in ordinary least squares regression models employing dynamic programming. The optimal position of these breaks can be determined by minimizing the residual sum of squares, and the optimal number of breaks can be determined by minimizing the Bayesian Information Criterion (Verbesselt *et al* 2010). The STL procedure and structural change analysis were implemented in R software using the *stl* and *breakpoints* functions available in the Forecast and Strucchange packages, respectively.

#### *2.3.3. Correlation analysis between NDVI dynamics and hydro–climatic factors*

The hydro–climatic effects on regional vegetation state tend to exhibit hysteresis (Piao *et al* 2014), and the intervals between two breakpoints vary from three to ten years according to regime shift detection results on the four variables. Thus partial correlation analysis

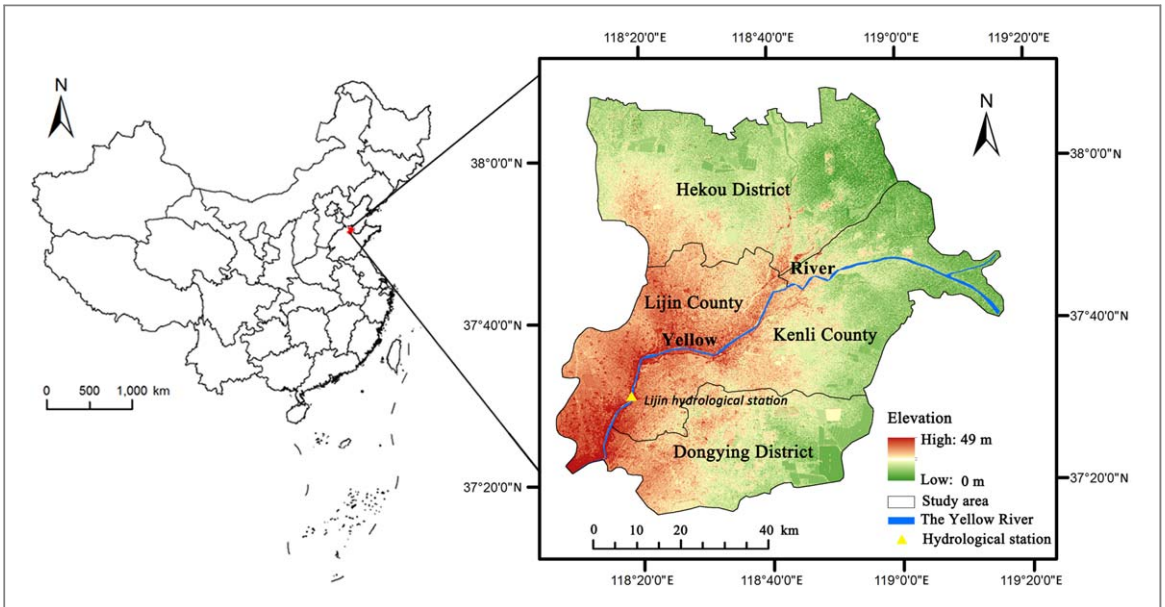


**Figure 1.** Sketch map of the Yellow River Delta based on elevation.

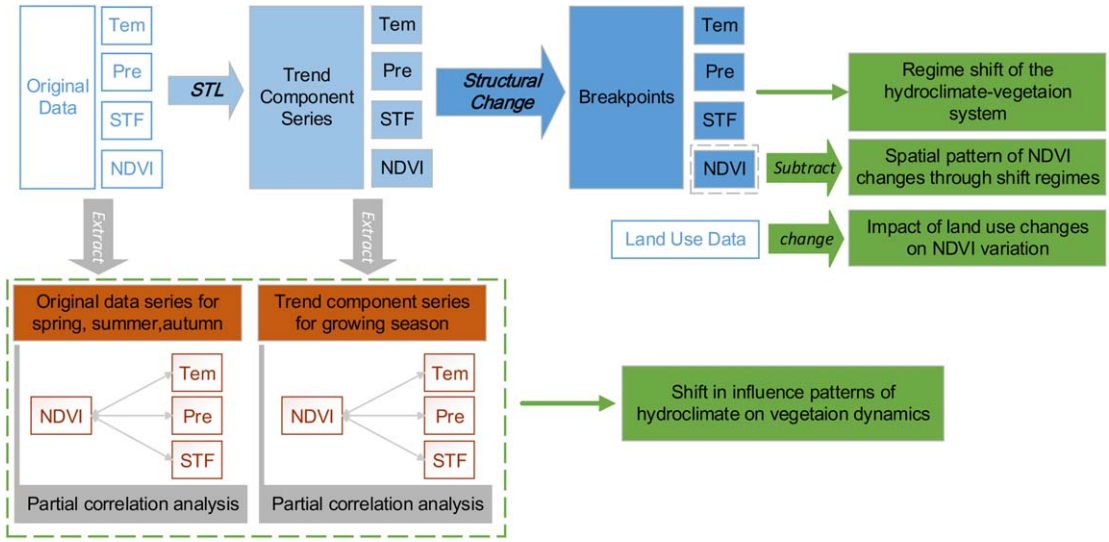


**Figure 2.** Method of analysis employed in this paper.

**Table 1.** Statistics of the Seasonal Kendall test for the hydro–climatic variables and NDVI in the Yellow River Delta during 1982–2015.

| | $Z_S$ | p value | Slope (unit/yr ) |
|---|---|---|---|
| TEM | 7.291 | 0.0000** | 0.040 °C |
| PRE | 0.424 | 0. 6718 | 0.011 mm |
| STF | −2.44 | 0.0147* | $-1.11 \times 10^7$ m$^3$ |
| NDVI | 7.712 | 0.0001** | 0.0012 |

$Z_S$: standardized normal variate; Slope: annual rate of change; ** significance at 1%; * significance at 5%.

was performed between NDVI and either TEM, PRE, and STF when the other two were fixed, employing a five-year moving window (e.g., the partial correlation coefficient of the year 2005 represents a moving window from 2003 to 2007) (Chu *et al* 2019). Observed data were used to calculate their correlations in spring (March–May), summer (June–August), and autumn (September–November). Since seasonality introduces pseudo-correlation between environmental variables due to synchronous climate conditions, the correlation analysis in the growing season (April–October) is based on the trend component.

The method of analysis is shown in figure 2.

## 3. Results

### 3.1. Long-term trends and regime shifts of hydroclimatic variables and NDVI

Seasonal Kendall test results show that areally averaged temperature exhibited significant increasing trends (at a rate of 0.040 °C yr$^{-1}$, $p < 0.01$), while no significant trend was revealed for the precipitation during 1982–2015 (table 1). The Yellow River streamflow at the Lijin hydrological station experienced a remarkable decrease (at a rate of $-1.11 \times 10^7$ m$^3$ yr$^{-1}$, $p < 0.05$). Besides this, a significant increasing trend of mean NDVI at a rate of 0.0012/yr ($p < 0.01$) was observed. On balance, the YRD presented a warmer–drier–greening trend during the study period.

The STL-decomposed trend series provides a more detailed display of temporal changes (figure 3(b)). Specifically, the temperature trend component rose in variability, and went through seven regimes with six breakpoints. During the first three phases, the average level gradually increased by about 2 °C, from 11.97 °C (January 1982–April 1988) through to 14.05 °C (June 1997–June 2002). It then fluctuated between 13.02 °C and 14.32 °C during the latter four phases. Despite no significant monotonic trend detected in the precipitation series the STL trend changes in the sub-series are evident, uncovering the transitions between precipitation states. Five breakpoints with six regimes were detected with alternate high–low levels corresponding to wet–dry transitional features. The trend of streamflow at the Lijin station displayed continuous reduction until the year 2003, when it began to recover. Specifically, the average annual streamflow declined from $3.31 \times 10^9$ m$^3$ to $4.5 \times 10^8$ m$^3$ during the first four phases, then it rebounded and remained at a level equal to $1.60 \times 10^9$ m$^3$ with slight oscillations. Concerning vegetation dynamics, the NDVI underwent five breakpoints defining six regimes (figure 3(b)). The average NDVI increased from 0.2463 (January 1982–May 1985) to 0.2946 (May 1999–August 2005), and after a temporary decline in phase IV, it ascended and reached a mean level equal to 0.3115 during September 2005–August 2012.

### 3.2. Correlation of NDVI dynamics and hydro–climatic factors

The NDVI correlated differently with temperature, precipitation, and streamflow, with obvious seasonal differences (figure 4). Notably, positive correlations between temperature and NDVI were detected for

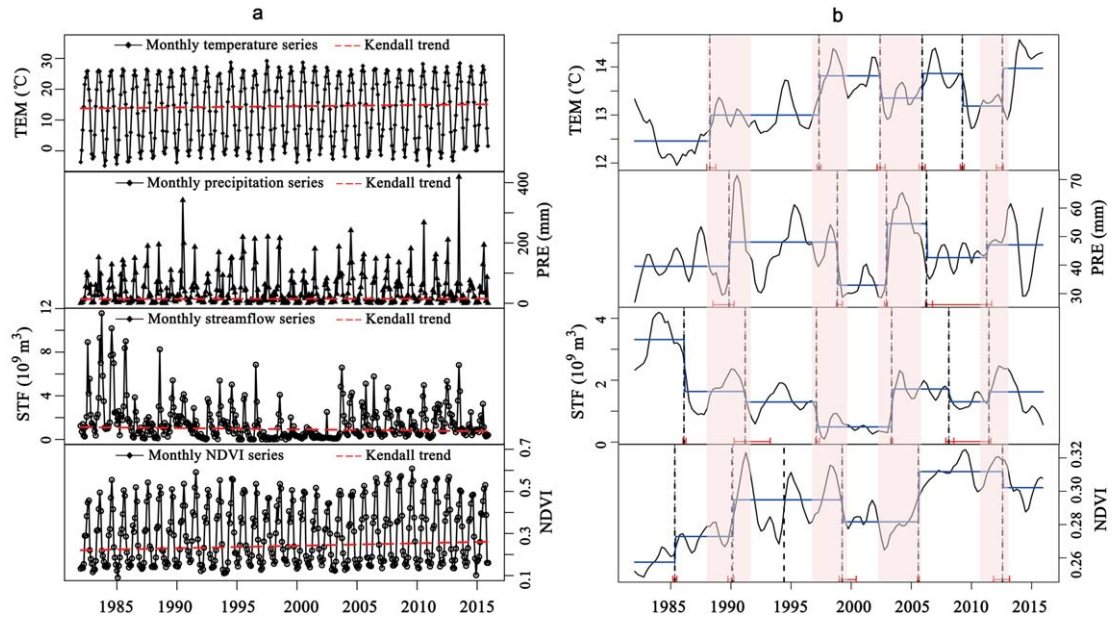


**Figure 3.** Temporal behavior of monthly average TEM, PRE, STF and NDVI (a), and corresponding STL-decomposed trends with regime shift dates (b). The vertical dashed lines show the breakpoints, with the bottom red segments indicating 95% confidence intervals. The pink strips cover periods during which the breakpoints in the time series are concentrated.

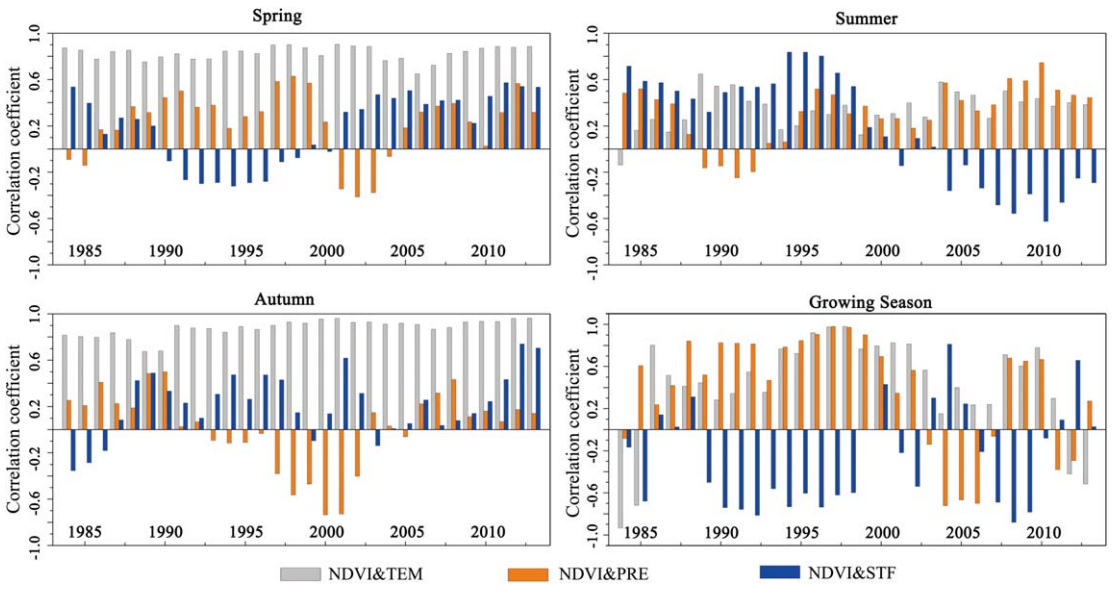


**Figure 4.** Partial correlation coefficient between NDVI and TEM ($P_{NDVI–TEM}$), PRE ($P_{NDVI–PRE}$), and STF ($P_{NDVI–STF}$) with a five-year moving window. Critical values of the correlation coefficient in the three seasons (spring, summer and autumn) are 0.4973, 0.5760, and 0.7080 at 0.1, 0.05, and 0.01 significant levels, respectively. Those in the growing season are 0.2913, 0.3440, and 0.4421, respectively.

almost all three seasons during the study period. Especially in spring and autumn, all partial correlations between the NDVI and temperature ($P_{NDVI–TEM}$) values were larger than 0.65 ($p < 0.05$), which confirmed temperature is the dominant factor promoting vegetative growth in these two seasons in the YRD. By comparison, correlation between precipitation and NDVI alternated between positive and negative values in different phases, with significant $P_{NDVI–PRE}$ only exhibited in particular short periods of each season, namely, positive during spring of 1997–1999, positive in summer 2004 and 2008–2011, and negative in the autumn of 1998–2001. It was determined that precipitation in spring during 1997–1999 (average 18.33 mm during the corresponding period 1995–2001) was clearly lower than the long-term mean seasonal value (average equal to 26.67 mm). This means precipitation in spring would be a major limiting factor of vegetative growth when it falls below a certain threshold. Streamflow impacted

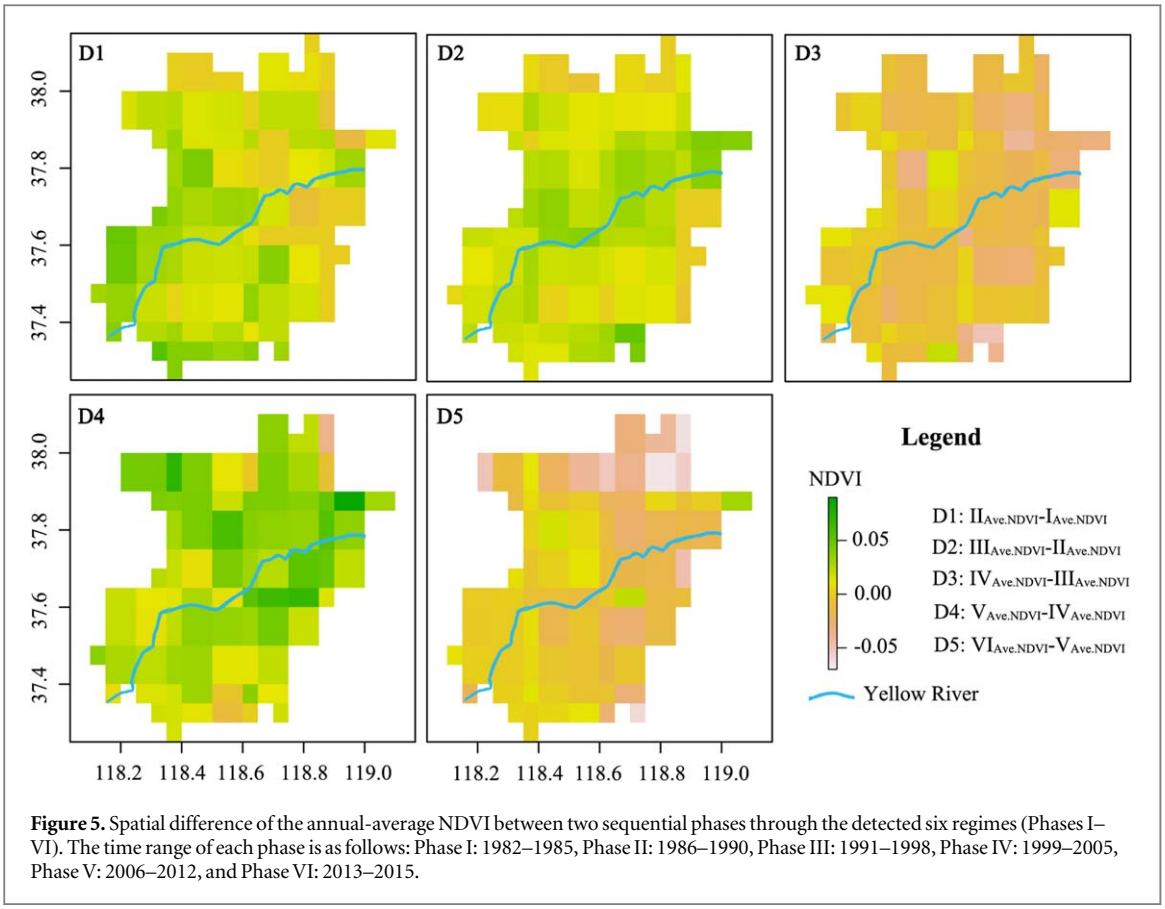


**Figure 5.** Spatial difference of the annual-average NDVI between two sequential phases through the detected six regimes (Phases I–VI). The time range of each phase is as follows: Phase I: 1982–1985, Phase II: 1986–1990, Phase III: 1991–1998, Phase IV: 1999–2005, Phase V: 2006–2012, and Phase VI: 2013–2015.

the NDVI mainly in summer, and the partial correlation coefficient between the NDVI and streamflow ($P_{NDVI–STF}$) was higher than the partial correlation coefficient between the NDVI and precipitation ($P_{NDVI–PRE}$) before about 1998; thereafter it became negative. It is herein concluded the relative large Yellow River streamflow before the construction of the Xiaolangdi Reservoir contributed to groundwater recharge and soil moisture to promote vegetative growth in spite of high evaporation. This pivotal role waned as a large quantity of streamflow was withheld by the reservoir.

During the growing season (figure 4) the $P_{NDVI–TEM}$ first increased from negative to positive and remained significantly positive ($p < 0.05$) during 1992–2003, with a continued rise during 2008–2010, and then became negative thereafter. The overall trend of $P_{NDVI–PRE}$ was generally similar to that of the $P_{NDVI–TEM}$, whereas $P_{NDVI–STF}$ was almost negative during the study period, except during three short periods (1986–1988, 2003–2005, and 2011–2013). In general, temperature and precipitation were the major and significant positive factors on vegetative growth, with streamflow mainly exerting a negative effect before about 2002. Thereafter the relatively stable relation was broken down.

### 3.3. Spatial variation of the NDVI and land use changes

*3.3.1. Spatial pattern of NDVI changes through six shift regimes*

Figure 5 depicts the spatial difference pattern of the annual-average NDVI between two sequential phases through the detected six regimes (Phases I–VI). Compared with Phase I (1982–1985) the increased NDVI in Phase II (1986–1990) occurred mainly in the southern part of the study area (figure 5(D1)). In Phase III (1991–1998), 96% of the study area exhibited enhanced NDVI, with larger increments (>0.02) mainly occurring in the riparian zone and central-north area (figure 5(D2)). During 1999–2005 (Phase IV) vegetation declined over most (82.4%, see figure 5(D3)) of the YRD. It recovered most along riparian zone of the Yellow River and the northern part of the study area during 2006–2012 (Phase V) (figure 5(D4)), followed by another widespread NDVI reduction in Phase VI (2013–2015) (figure 5(D5)). Generally, the NDVI varied in most parts of the YRD in the same sense (increasing or decreasing) through sequential phases due to similar hydroclimatic conditions, which caused shifts in the vegetative state. Observed anomalies in the NDVI might be caused by soil salinization induced by seawater intrusion and by land use/cover changes.

**Table 2.** Land use distribution within the study area in 1980, 2000, and 2015.

| Type | Area ($km^2$) | | |
|---|---|---|---|
| | 1980 | 2000 | 2015 |
| Paddy fields | 170 | 221 | 209 |
| Dry farmland | 2264 | 2496 | 3063 |
| Forest | 20 | 22 | 43 |
| Grassland | 933 | 1088 | 518 |
| **Vegetation area** | **3387** | **3827** | **3833** |
| Water | 770 | 527 | 592 |
| Built-up land | 583 | 849 | 1016 |
| Saline land | 953 | 592 | 374 |
| Unused land | 137 | 161 | 139 |
| **Non-vegetation area** | **2443** | **2129** | **2121** |

*3.3.2. Land use changes and its impact on NDVI variation*

During 1980–2015 the vegetative coverage area in the YRD increased by 13.17%, where dry farmland was the primary land use type accounting for 38.83% of the study area in 1980, and for 51.44% in 2015 (table 2). Built-up land was the fastest growing land use type (increasing rate of 74.27%), yet its total area was about one third of that occupied by dry farmland in 2015. The increase in farmland mainly accrued from conversion of grassland and saline land. In a spatial sense the increment of vegetated area occurred mainly in the north-eastern part of the study area, most of it along the estuarine wetland and coastline during 1980–2000 (figure 6(a)). During 2000–2015 farmland increased rapidly mainly in the northeastern part of the study area (figure 6(b)). The observed increase in NDVI is confined to the northeastern part of the study area, with a minor increase of NDVI along the Yellow River. This means the direct effect of land use change on regional vegetation is more local in the YRD compared to hydroclimatic influences. The large expansion in farmland was a major contributor to the regional increase of the NDVI. Compared to grassland and saline land farmland can increase the maximum value of the growing-season NDVI at sites with good management measures (Jiang *et al* 2013).

## 4. Discussion

### 4.1. Regime shift of the hydroclimate-vegetation system in the Yellow River Delta

The breakpoints of the four STL-decomposed trends indicate there existed four relative uniform transition periods of the hydro–climatic variables and NDVI (figure 3(b), pink strip covered periods), which are roughly centered on the years 1989, 1998, 2004, and 2012. It is concluded the YRD experienced four regime shifts in its hydroclimate–vegetation system during 1982–2015. At the regional scale TEM, PRE, and NDVI increased from 1980s through 1990s, indicating the YRD experienced warmer–wetter climate and lusher vegetation. TEM increased by 1.04°C after 1998 while PRE and STF declined sharply, causing warmer–dryer conditions. Therefore, the NDVI declined mainly due to increased high-temperature induced evaporation and less water replenishment from precipitation and streamflow. During the third transition period TEM decreased and PRE increased, coupled with significantly improved streamflow caused by water replenishment. This constitutes suitable environmental conditions favoring continuous recovery of vegetation. In 2012 the hydroclimate–vegetation system exhibited a similar pattern to that of the second transition period in 1998.

Regime shift occurrence is expected to increase as human influence on earth increases, including human-induced climate change and hydrologic change. Regime shift in temperature and precipitation within the YRD occurred once every 7–10 years before 2000; thereafter, the occurrence increased to once every 3–5 years (figure 3). By comparison, streamflow has been varying at a relative high frequency of once per 4–6 years during 1982–2015, due to continuous external pressures (e.g. reduction of the source water, increased water consumption, and hydrological regulation; more details are provided in the supplementary material). Vegetation dynamics in the YRD reflect the integrated environmental changes including hydroclimate changes and human-induced changes on land use/cover, groundwater storage, and soil properties. As a result, the duration of each NDVI regime varied in a larger range of 4–9 years.

### 4.2. Shift in the influence of hydroclimatic variables on the NDVI

Influences of hydroclimate on vegetation growth can shift and be positive or negative, depending on their relative status. For example, increasing temperatures in temperature-limited ecosystems can first support vegetation growth that results in greening NDVI trends, while a further warming can induce drought stress that slightly turns the initial greening to a browning trend (Forkel *et al* 2013). During the first shift period (around 1989), precipitation contributed more ($P_{NDVI–PRE} > 0.82$, $p < 0.01$) than temperature (no significant $P_{NDVI–TEM}$) to the increment of NDVI. The streamflow began to exhibit significant negative impact ($-0.81 < P_{NDVI–PRE} < -0.50$), particularly in spring seasons of the period 1990–1998, despite not being statistically significant (figure 4). After the second shift period (about 1998), the positive role of precipitation weakened substantially due to its substantial decline (figure 3(b), monthly average rainfall of the third regime declined by 15.11 mm compared to that of the previous regime). Rising regional temperature and reduced rainfall constitute major factors limiting vegetation growth in spring and autumn (figure 4). Streamflow has been drastically reduced due to reservoir construction. Nevertheless, streamflow

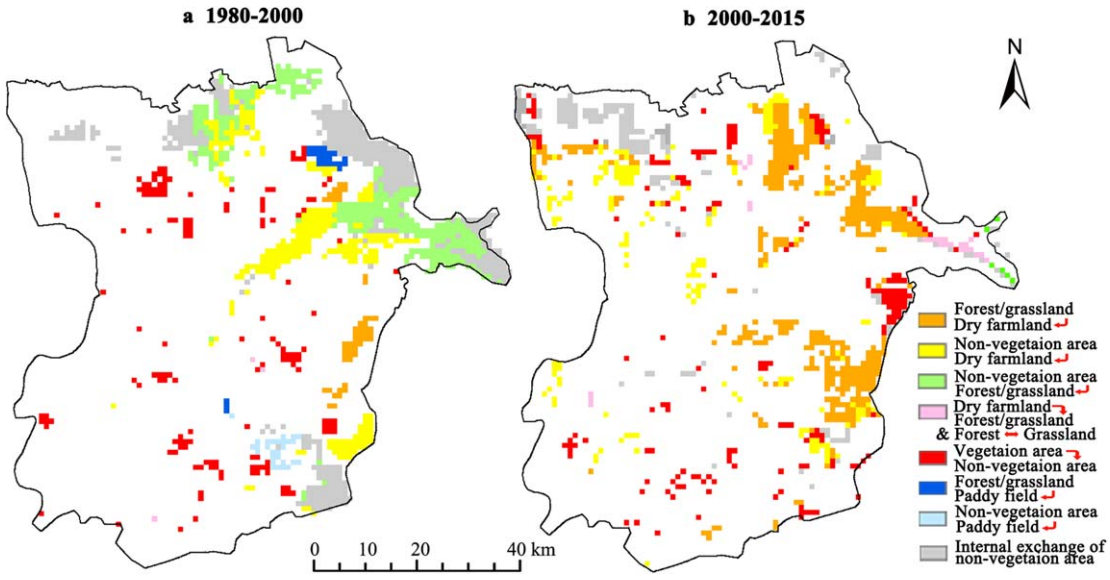


**Figure 6.** Land use change map (a) from 1980 through 2000 and (b) from 2000 through 2015.

began to play an important role on vegetative water procurement via discharge to groundwater in spring and autumn. The rapid short-term fluctuations of temperature and precipitation during the third shift period (around 2004) cause their influence on the NDVI to shift between positive and negative. The enhanced streamflow contributes largely to the greening trend ($P_{NDVI-STF} = 0.81$), while there was a significant negative effect due to the drastic reduction of precipitation ($\sim -0.70$). The last regime after the fourth shift period experienced an extreme drought condition exceeding the threshold of vegetation growth for hydrothermal conditions, which stems from the negative effects of temperature and precipitation. Again, streamflow played a central role in maintaining vegetation growth.

Temperature is the dominant factor on vegetation growth in the YRD where the significant increasing spring and winter temperatures account for the lengthening of the growing season and enhancement of photosynthesis, and prompted the greening trend (Piao *et al* 2014). Precipitation is a limiting factor, whose effect on vegetation depends on the variation of temperature. The short-term extreme drought event (around 1998, 2005, and 2012) is likely to cause the negative effect of precipitation on vegetation due to the insufficient rainfall relative to high temperature. Streamflow is either a limiting or complementary factor. The extreme low streamflow in spring ($3.48 \times 10^8$ during 1992–1996 corresponding to the last and first years of the five-year windows indicated by 1990 and 1998, respectively) could cause groundwater to discharge to the river. Furthermore, depleted groundwater induced seawater intrusion and accelerated salinization of groundwater (Fan *et al* 2012). Low streamflow and groundwater depletion seriously endangered the health of the regional vegetation and ecosystem. Streamflow may act as an important water supply factor for vegetation growth when the drought extent of regional climate exceeds a threshold in the YRD. The threshold varies across different regime states depending on the relative status of temperature, precipitation, and evapotranspiration. The manner in which hydroclimate variables may coalesce to determine such threshold calls for further studies to guide water use within the Yellow River Basin.

### 4.3. Implications of environmental system shifts in larger regions

Satellite data indicate increasing greenness over the Earth's lands since the early 1980s, with greening in China being the most notable, mainly occuring in the eastern region (Chen *et al* 2019). The greening of the Central Plains region of China is mainly contributed by cropland, which confirms our results that the expansion of farmland was a major contributor to the regional increase of the NDVI in YRD. Looking at a wider region—the lower Yellow River Basin (figure S1 is available as part of the online supplementary material, at stacks.iop.org/ERL/15/024017/mmedia)—similar trends in regional average TEM (significant increasing at a rate of 0.03 °C $yr^{-1}$), PRE (no significant trend), and NDVI (significant increasing at a rate of 0.002/yr) were detected. Regarding the regime shifts breakpoints of the STL-decomposed trends of TEM, PRE and NDVI during 1982–2015 are not always in agreement or synchronous, yet, there are three uniform transition periods (roughly centered on the years 1998, 2003, and 2012) (figure S2). We can infer that the larger the region, the more widespread the disturbances (e.g., different climate change zones, land type changes, etc); therefore, it is difficult to identify a unified regime shift. After 2005 the YRD and the lower Yellow River Basin exhibited a significant increase in

NDVI driven by increased cropland, and by the water–sediment regulation scheme by the Yellow River Conservancy Commission. A more detailed and flexible regulation scheme is urgently needed to guarantee social and ecological sustainability, hence, we suggest developing a real-time scenario model to guide water–sediment regulation. Specifically, based on the state of the system and climatic conditions the water demand of downstream crops, plants, wetlands, economic production, and urban use must be accounted for to lead to a scientific basis for real-time river water regulation and supply.

## 5. Conclusion

This study has assessed the regime shifts of the regional hydroclimate–vegetation system in the Yellow River Delta (YRD). Our findings indicate the YRD featured a significant warmer–drier–greening trend during 1982–2015. Four relative uniform shift periods of regional temperature, precipitation, streamflow and NDVI series, roughly centered in 1989, 1998, 2004, and 2012, respectively, were identified establishing that the YRD experienced four regime shifts of its hydroclimate–vegetation system during 1982–2015.

Temperature was the dominant factor promoting seasonal vegetative growth in spring and autumn (all $P_{NDVI-TEM}$ were greater than 0.65), and streamflow impacted the NDVI mainly in summer. Temperature and precipitation were the dominant interannual controls on vegetative growth in the growing season before 2002. Subsequently, precipitation and streamflow alternately became the main moisture influencing factors on vegetative growth. Streamflow played an important complementary role on vegetation when the drought extent exceeds a certain threshold in the YRD. Moreover, the climate state shift determined the spatial changes of NDVI. Streamflow mainly contributed to vegetative growth in the riparian zone. Land use change plays a positive role in the northeastern part of the study region, where the vegetated area increased the most. The results of this paper improve our understanding of regime shifts of the hydroclimate–vegetation system of the YRD during the past 34 years, and the role of streamflow on the regional environmental system. This improved understanding could assist water management and climatic adaptation in the YRD.

## Acknowledgments

This research was supported by National Natural Science Foundation of China (Grant No. 41807004) and project funded by China Postdoctoral Science Foundation (Grant No. 2017M622237).

## Data availability statements

The data that support the findings of this study are available from the corresponding author upon reasonable request.

## References

Andersen T, Carstensen J, Hernández-García E and Duarte C M 2009 Ecological thresholds and regime shifts: approaches to identification *Trends Ecol. Evol.* **24** 49–57

Burrell A L, Evans J P and Liu Y 2017 Detecting dryland degradation using time series segmentation and residual trend analysis (TSS-RESTREND) *Remote Sens. Environ.* **197** 43–57

Chen C *et al* 2019 China and India lead in greening of the world through land-use management *Nat. Sustain.* **2** 122–9

Chu H, Venevsky S, Wu C and Wang M 2019 NDVI-based vegetation dynamics and its response to climate changes at Amur-Heilongjiang River Basin from 1982 to 2015 *Sci. Total Environ.* **650** 2051–62

Cleveland R B, Cleveland W S, McRae J E and Terpenning I 1990 STL: a seasonal-trend decomposition procedure based on loess *J. Off. Stat.* **6** 3–33 ((https://www.wessa.net/download/stl.pdf))

Fan X, Pedroli B, Liu G, Liu Q, Liu H and Shu L 2012 Soil salinity development in the yellow river delta in relation to groundwater dynamics *L. Degrad. Dev.* **23** 175–89

Fensholt R, Nielsen T T and Stisen S 2006 Evaluation of AVHRR PAL and GIMMS 10-day composite NDVI time series products using SPOT-4 vegetation data for the African continent *Int. J. Remote Sens.* **27** 2719–33

Fensholt R and Proud S R 2012 Evaluation of earth observation based global long term vegetation trends-comparing GIMMS and MODIS global NDVI time series *Remote Sens. Environ.* **119** 131–47

Forkel M, Carvalhais N, Verbesselt J, Mahecha M D, Neigh C S R and Reichstein M 2013 Trend change detection in NDVI time series: effects of inter-annual variability and methodology *Remote Sens.* **5** 2113–44

Groß E, Mård J, Kalantari Z and Bring A 2018 Links between Nordic and Arctic hydroclimate and vegetation changes: contribution to possible landscape-scale nature-based solutions *L. Degrad. Dev.* **29** 3663–73

Guo X, Zhang H, Wu Z, Zhao J and Zhang Z 2017 Comparison and evaluation of annual NDVI time series in China derived from the NOAA AVHRR LTDR and terra MODIS MOD13C1 products *Sensors* **17** 1298

Hagenlocher M, Renaud F G, Haas S and Sebesvari Z 2018 Vulnerability and risk of deltaic social-ecological systems exposed to multiple hazards *Sci. Total Environ.* **631–632** 71–80

Harrison G W 1979 Stability under environmental stress: resistance, resilience, persistence, and variability *Am. Nat.* **113** 659–69

Hirsch R M and Slack J R 1984 A nonparametric trend test for seasonal data with serial dependence *Water Resour. Res.* **20** 727–32

Holben B 1986 Characteristics of maximum-value composite images from temporal AVHRR data *Int. J. Remote Sens.* **7** 1417–34

Hu M and Xia B 2019 A significant increase in the normalized difference vegetation index during the rapid economic development in the Pearl River Delta of China *L. Degrad. Dev.* **30** 359–70

Hua Y, Cui B, He W and Cai Y 2016 Identifying potential restoration areas of freshwater wetlands in a river delta *Ecol. Indic.* **71** 438–48

Ibrahim Y Z, Balzter H, Kaduk J and Tucker C J 2015 Land degradation assessment using residual trend analysis of GIMMS NDVI3g, soil moisture and rainfall in Sub-Saharan West Africa from 1982 to 2012 *Remote Sens.* **7** 5471–94

Jiang C, Pan S and Chen S 2017 Recent morphological changes of the Yellow River (Huanghe) submerged delta: causes and environmental implications *Geomorphology* **293** 93–107
Jiang D, Fu X and Wang K 2013 Vegetation dynamics and their response to freshwater inflow and climate variables in the Yellow River Delta, China *Quat. Int.* **304** 75–84
Jiapaer G, Liang S, Yi Q and Liu J 2015 Vegetation dynamics and responses to recent climate change in Xinjiang using leaf area index as an indicator *Ecol. Indic.* **58** 64–76
John R, Chen J, Ou-Yang Z T, Xiao J, Becker R, Samanta A, Ganguly S, Yuan W and Batkhishig O 2013 Vegetation response to extreme climate events on the Mongolian Plateau from 2000 to 2010 *Environ. Res. Lett.* **8** 035033
Kong D, Miao C, Borthwick A G L, Duan Q, Liu H, Sun Q, Ye A, Di Z and Gong W 2015 Evolution of the Yellow River Delta and its relationship with runoff and sediment load from 1983 to 2011 *J. Hydrol.* **520** 157–67
Koster R D, Walker G K, Collatz G J and Thornton P E 2014 Hydroclimatic controls on the means and variability of vegetation phenology and carbon uptake *J. Clim.* **27** 5632–52
Lafare A E A, Peach D W and Hughes A G 2015 Use of seasonal trend decomposition to understand groundwater behaviour in the Permo-Triassic Sandstone aquifer, Eden Valley, UK *Hydrogeol. J.* **24** 141–58
Liu B, Peng S, Liao Y and Long W 2018a The causes and impacts of water resources crises in the Pearl River Delta *J. Clean. Prod.* **177** 413–25
Liu H, Gao C and Wang G 2018b Understand the resilience and regime shift of the wetland ecosystem after human disturbances *Sci. Total Environ.* **643** 1031–40
Liu S, Hou X, Yang M, Cheng F, Coxixo A, Wu X and Zhang Y 2018c Factors driving the relationships between vegetation and soil properties in the Yellow River Delta, China *Catena* **165** 279–85
Lu Q, Kang L, Shao H, Zhao Z, Chen Q, Bi X and Shi P 2016 Investigating Marsh sediment dynamics and its driving factors in Yellow River delta for wetland restoration *Ecol. Eng.* **90** 307–13
Piao S *et al* 2014 Evidence for a weakening relationship between interannual temperature variability and northern vegetation activity *Nat. Commun.* **5** 5018
Sarkkola S, Koivusalo H, Laurén A, Kortelainen P, Mattsson T, Palviainen M, Piirainen S, Starr M and Finér L 2009 Trends in hydrometeorological conditions and stream water organic carbon in boreal forested catchments *Sci. Total Environ.* **408** 92–101
Shi L, Wang Y, Jia Y, Lu C, Lei G and Wen L 2017 Vegetation cover dynamics and resilience to climatic and hydrological disturbances in seasonal floodplain: the effects of hydrological connectivity *Front. Plant Sci.* **8** 2196
Stow C A, Cha Y, Johnson L T, Confesor R and Richards R P 2015 Long-term and seasonal trend decomposition of Maumee River nutrient inputs to western Lake Erie *Environ. Sci. Technol.* **49** 3392–400
Verbesselt J, Hyndman R, Newnham G and Culvenor D 2010 Detecting trend and seasonal changes in satellite image time series *Remote Sens. Environ.* **114** 106–15
Walker B and Salt D 2006 *Resilience Thinking: Sustaining Ecosystems and People in a Changing World* (Washington, DC: Island Press)
Wei Y, Jiao J, Zhao G, Zhao H, He Z and Mu X 2016 Spatial-temporal variation and periodic change in streamflow and suspended sediment discharge along the mainstream of the Yellow River during 1950-2013 *Catena* **140** 105–15
Wen Z, Wu S, Chen J and Lü M 2017 NDVI indicated long-term interannual changes in vegetation activities and their responses to climatic and anthropogenic factors in the Three Gorges Reservoir Region, China *Sci. Total Environ.* **574** 947–59
Xu H J, Wang X P and Yang T B 2017 Trend shifts in satellite-derived vegetation growth in Central Eurasia, 1982–2013 *Sci. Total Environ.* **579** 1658–74
Yu J, Chen X, Sun Z, Xie W, Mao P, Chunfa W U, Dong H, Xiaojie M U, Yunzhao L I and Guan B 2010 The spatial distribution characteristics of soil nutrients in new-born coastal wetland in the Yellow River delta *Acta Sci. Circumstantiae* **30** 855–61
Zhou Y, Huang H Q, Nanson G C, Huang C and Liu G 2015 Progradation of the Yellow (Huanghe) River delta in response to the implementation of a basin-scale water regulation program *Geomorphology* **243** 65–74
Zhu L and Southworth J 2013 Disentangling the relationships between net primary production and precipitation in Southern Africa Savannas using satellite observations from 1982 to 2010 *Remote Sens.* **5** 3803–25